Silicon (2019) 11:117–135
https://doi.org/10.1007/s12633-018-9836-x

ORIGINAL PAPER

Effects of the Nanoclay and Crosslinking Systems on the Mechanical Properties of Ethylene-propylene-diene Monomer/styrene Butadiene Rubber Blends Nanocomposite

S. Vishvanathperumal[1] · **S. Gopalakannan**[1]

Received: 28 October 2017 / Accepted: 27 March 2018 / Published online: 7 April 2018

Abstract
This paper investigates the effect of nanoclay and crosslinking systems on the cure characteristics, mechanical properties, abrasion resistance, compression set and swelling properties of ethylene-propylene-diene monomer (EPDM)/styrene butadiene rubber (SBR) blends. Nanocomposites were prepared by two-roll mill. In this work, three different crosslinking systems were used, namely, sulphur, dicumyl peroxide and the mixed system consisting of sulphur and peroxide. The mechanical properties such as tensile strength, elongation at break, 100% modulus, hardness, crosslink density and tear strength of the EPDM/SBR nanocomposites were studied. Cure study indicates that nanoclay not only accelerates the curing reactions but also gives rise to a noticeable increase of the torque values, representing crosslinking density of the nanocomposites increases at the existence of nanoclay. The tensile strength and 100% modulus of EPDM/SBR nanocomposites increases with increase in nanoclay content up to 7.5 phr and then decreases for all the different crosslinking system. The elongation at break, hardness, tear strength and compression set increases with increasing content of nanoclay.

Keywords Ethylene-propylene-diene monomer · Styrene butadiene rubber · Nanoclay · Crosslinking systems · Mechanical properties

1 Introduction

Composite materials are generally made up of two distinct phases; matrix phase and other the reinforcement phase. The reinforcement phase usually has a higher strength and modulus than the polymer matrix and is generally fibre or particles form. One of the greatest innovative development and successful growths in polymer composite is the innovation of polymer nanocomposites [1–3]. Nanoclay (NC) based polymer nanocomposites were studied intensively by numerous research group in recent years. Clays as well as clay minerals such as montmorillonite, hectorite, saponite, etc, were widely used as filler materials for rubber and plastic for several years and saving polymer consumption as well as the cost reduced [4–7].

Montmorillonite (MMT) is the most commonly used layered silicate and it occurs naturally. Polymer-layered silicate nanocomposites have significant improvement in mechanical, thermal and barrier properties at very low concentration [8–10]. Montmorillonite has the large surface area, high cation exchange capacity and high aspect ratio [11]. The nanoclay is inorganic in nature and is incompatible with the organic polymer matrices due to hydrophilic. MMT clays are converted into organophilic (hydrophobic) so as to give good compatibility with the polymer matrix since most of the polymers are hydrophobic. For making the layered silicate filler compatible with the organic polymer, the silicate layer surfaces are organically modified by exchanging the alkali cations to alkyl ammonium ions [12–14]. The modifications of the layered silicate fillers have the significant advantage in the mechanical, thermal and barrier properties of the polymer nanocomposites [15, 16].

✉ S. Vishvanathperumal
vishvamechanical@gmail.com

S. Gopalakannan
gopalakannan75@gmail.com

[1] Department of Mechanical Engineering, Adhiparasakthi Engineering College, Melmaruvathur, Tamilnadu, 603319, India

In recent years, polymer/clay nanocomposites (PCNs) have emerged as a new class of materials. PCNs were first discovered as well as developed by the Toyota research group [2]. However, very fewer works have been carried out on rubber/clay (RCNs) nanocomposites. Nowadays, elastomer materials are widely used in the polymer industry, ranging from automotive to domestic applications. The growth of RCNs would be a positive advantage to the rubber engineering works because of the improved physical properties. The dispersion of lesser amount of clay in the polymer matrix can impart essential improvement in mechanical properties (tensile and tear strength, tensile modulus, and hardness), solvent resistance, gas barrier properties, ionic conductivity, flammability resistance and biodegradability of polymers. Many researchers have already worked on PCNs based on a variety of polymers, i.e. natural rubber [17, 18], styrene butadiene rubber [19, 20], ethylene propylene diene rubber [21], etc.

SBR is a widely used rubber and it is the first synthetic rubber considered for manufacturing the rubber materials because of its low price. SBR, despite around good mechanical properties particularly abrasion resistance and is sensitive to the environmental factors such as moisture, ozone, light, and heat due to the presence of double bonds in the main chain. This weakness would be altered by SBR blended with highly saturated elastomers like EPDM. EPDM is an excellent special purpose rubber used in wide variety of applications. EPDM rubbers exhibit superior oxidative and ozone, weather and heat resistance due to the substantial absence of unsaturation in polymer backbone [22, 23].

Size, structure and the aspect ratio of the filler affect processability and vulcanisation of elastomers. Clays, widely used in rubber industry for their low cost and accessibility, improve abrasion resistance, mechanical strength, and heat distortion of rubbers. These outstanding properties of clay might be attributed to its high aspect ratio. This is primarily attributed to the nanoscale dimension of layered silicate dispersed in the matrix which causes a strong interfacial interaction between polymer chains and layered silicate, most important to a significant change in the mechanical strength, thermal stability, dynamic mechanical properties, optical, barrier properties and fire resistance compared to properties of their conventional filled polymers [24–26]. Crosslink density is an important parameter and it affects the physical, mechanical and viscoelastic properties of the composites [27–29]. The effect of blend ratio on crosslinking behaviour and dynamic elastic properties of EPDM and high-density polyethylene (HDPE) blends was studied by a torque rheometer. They found that the crosslink density increases and then decrease with an increase in the content of EPDM [30]. The mechanical properties and ozone resistance increase with increasing content of EPDM. The tensile strength, hardness, abrasion resistance, complex viscosity, storage modulus and ozone resistance of SBR/EPDM/Cloisite 20A composites increases with increasing content of nanoclay [31].

The effects of blend ratio, cure systems and fillers on the mechanical properties of EPDM/SBR blends. They found that morphology studies of the blends show the existence of excellent interphase between EPDM and SBR in the blend ratio 80:20. The mixed system on the tensile and tear strengths of the EPDM/SBR blends is higher compared to the sulphur and DCP systems but the elongation at break is higher for sulphur cured system [32]. The effect of a vulcanising system on cure and mechanical properties of acrylonitrile butadiene rubber (NBR)/EPDM blends are investigated [33]. The cure characteristics exhibit much higher elasticity for the base NBR and rich NBR rubber blend (SBR/NBR, 20/80) with Cloisite30B than Cloisite15A because of the greater affinity between NBR and Cloisite 30B. The cure characteristics exhibit much higher elasticity for the base SBR and rich SBR rubber blend (SBR/NBR, 80/20) with Cloisite15A than Cloisite30B [34]. The elongation at break decreases with increase in the content of nanoclay whereas hardness increases gradually up to 3 wt.% for natural rubber (NR)/SBR rubber blend [35]. The minimum torque, maximum torque, delta torque and optimum cure time are increased, but scorch time and cure rate index are decreased with the increased content of carbon black in the NBR/EPDM blend. The tensile strength and hardness are increased, but elongation at break decreased with increasing the content of carbon black for all NBR/EPDM blends [36].

The objective of the research work is to prepare the blends of ethylene-propylene-diene monomer and poly (styrene-co-butadiene) rubber filled with nanoclay and to study the effect of nanoclay (Cloisite 30B) loading and crosslinking systems on the mechanical properties of unaged and aged EPDM/SBR rubber blends. This paper also reflects the effect of crosslinking systems and nanoclay loading in EPDM/SBR rubber blend on the cure characteristics, compression set, and morphology.

2 Experimental

2.1 Materials

Ethylene-propylene-diene monomer - EPDM (KEP 270), Mooney viscosity (ML (1 + 4) 125 °C) 60 M, ethylene content 68 wt.%, termonomer content (ethylidene norbornene) 4.5%, density 0.86 g/cm^3 and styrene butadiene rubber (SBR-1502), styrene content 23 wt.%, Mooney viscosity (ML (1 + 4) 100 °C) 52 M, density 0.93 g/cm^{3}was procured from Arihant Reclamation Private Limited,

Delhi, India. Cloisite 30B (organo-modified layered nanosilicates), modifier concentration cation exchange capacity of 90 meqv./100 g clay, methyl-tallow-bis (hydroxyethyl)-ammonium treated montmorillonite was procured from Southern Clay Products, USA. The rubber chemicals used such as zinc oxide, stearic acid, mercapto benzothiazyl disulphide (MBTS), tetramethyl thiuram disulphide (TMTD), sulphur and dicumyl peroxide were of commercial grade.

2.2 Preparation of Nanocomposites

The nanocomposite was prepared in two roll mixing mill operated at 80 °C having a friction ratio of 1:1.4. EPDM was masticated for 4 min and blended with SBR for about 4 min. After the homogenisation of the EPDM/SBR rubber blend (for about 8 min) and then nanoclay and curatives were added orderly according to ASTM D15 [37]. The compounding formulations of the nanocomposites are given in Table 1. The three different crosslinking systems are sulphur (S), dicumyl peroxide (DCP) and the mixed system consisting of sulphur and dicumyl peroxide (S +DCP) are indicated as S, P and M respectively. The nanocomposites containing sulphur system are labelled as S_0 (80/20/0 EPDM/SBR/NC), $S_{2.5}$ (80/20/2.5 EPDM/SBR/NC), S_5 (80/20/5 EPDM/SBR/NC) and so on. Similarly, the nanocomposites containing dicumyl peroxide and mixed systems are labelled, respectively, as P_0 and M_0 (80/20/0 EPDM/SBR/NC) $P_{2.5}$ and $M_{2.5}$ (80/20/2.5 EPDM/SBR/NC), P_5 and M_5 (80/20/5 EPDM/SBR/NC) and so on. The cure characteristics of the EPDM/SBR/NC blends were studied with an oscillating disc rheometer. The compounded blends were moulded into sheets of 2 mm thickness using an electrically heated hydraulic press under a pressure of 30 MPa at a 160 °C and at an optimum curing time.

2.3 Characterisation

2.3.1 Rheometric Characteristic

The rheological test of unvulcanized rubber samples was carried out according to ASTM D-2084 by the oscillating disc rheometer under 160 °C, oscillation arc 0.5° and 100 cycles per minutes (1.66 Hz) testing conditions. Minimum torque (M_l), maximum torque (M_h), scorch time (t_{S2} – the period in the curve in which the minimum torque increase by two Mooney units [38]), optimum curing time (t_{90} – the period in the curing curve where 90% increase in torque [38]) and cure rate index (CRI) are measured. CRI was calculated using the equation.

$$CRI = \frac{100}{optimum\ curetime - scorchtime} \quad (1)$$

2.3.2 Mechanical Properties

Tensile and tear properties were performed at 23 °C respectively, on dumbbell- and un-nicked 90° angle test-shaped specimens according to ASTM standards D 412-C and D 624-B on a universal testing machine - series 7200 by Dak System Inc (model: T-72102) at a crosshead

Table 1 Formulation for EPDM/SBR/NC rubber blends

Crosslinking system types	Sample code	Compounds (phr)								
		EPDM	SBR	Clay	Zinc oxide	Stearic acid	MBTS	TMTD	Sulphur	Dicumyl peroxide
Sulphur system	S_0	80	20	0	4	1.5	1.2	1	2.5	-
	$S_{2.5}$	80	20	2.5	4	1.5	1.2	1	2.5	-
	S_5	80	20	5	4	1.5	1.2	1	2.5	-
	$S_{7.5}$	80	20	7.5	4	1.5	1.2	1	2.5	-
	S_{10}	80	20	10	4	1.5	1.2	1	2.5	-
Peroxide system	P_0	80	20	0	-	-	-	-	-	4
	$P_{2.5}$	80	20	2.5	-	-	-	-	-	4
	P_5	80	20	5		-	-	-	-	4
	$P_{7.5}$	80	20	7.5	-	-	-	-	-	4
	P_{10}	80	20	10	-	-	-	-	-	4
Mixed systems	M_0	80	20	0	4	1.5	1.2	1	2.5	4
	$M_{2.5}$	80	20	2.5	4	1.5	1.2	1	2.5	4
	M_5	80	20	5	4	1.5	1.2	1	2.5	4
	$M_{7.5}$	80	20	7.5	4	1.5	1.2	1	2.5	4
	M_{10}	80	20	10	4	1.5	1.2	1	2.5	4

speed of 500 mm/min. Hardness is measured with a Shore-A Durometer as per ASTM D-2240. The average of five readings is reported for each sample. Tensile (tensile strength, elongation at break and 100% modulus) test samples, tear and hardness test samples were heated at 100 °C in an air circulating oven for 96 hours. The sample is then cooled down for 30 minutes and conditioned at room temperature. The dimensions of each sample were measured and tested.

2.3.3 Crosslinking Density

The degree of crosslinking density has been calculated by the following equation [39, 66, 67].

$$v(\frac{mol}{cm^3}) = \frac{1}{2M_c} \tag{2}$$

where M_c is the molar mass of the polymer between crosslinks. Molar mass between the crosslinks of the nanocomposites has been calculated from the Flory-Rehner equation [39, 65–67].

$$M_c(\frac{g}{mol}) = \frac{-\rho_p V_s V_r^{1/3}}{\ln(1-V_r) + V_r + \chi V_r^2} \tag{3}$$

where, ρ_p is the density of the polymer, V_s is the molar volume of the solvent (106.3 mL/gmol), V_r is the volume fraction of polymer in the solvent-swollen filled compound, χ is the interaction parameter of the polymer (0.3) [68], and V_r is given by following equation [69]

$$V_r = \frac{1}{1+Q_m} \tag{4}$$

where, Q_m is the weight swell of the EPDM/SBR nanocomposites in toluene.

2.3.4 Rebound Resilience

The rebound resilience of the nanocomposites was carried out according to the ASTM D 2632. In this method, a plunger suspended from a given height above the specimen was released and the rebound height was determined. The ratio of the rebound height and the original height is stated to as the rebound resilience and expressed as a percentage. The test was performed on the vertical rebound tester as resiliometer. The average of five readings is reported for each sample.

2.3.5 Abrasion Resistance

Abrasion resistance of the rubber nanocomposites in terms of volume loss was determined on DIN abrader (Zwick Abrasion tester, model 6102) according to DIN 53516, ASTM D5963 and ISO 4649. The cylindrical shape specimen (10 ± 0.2 mm in diameter and 12 ± 0.2 mm in thickness) was placed in the starting position of the DIN abrader testing machine. After, the specimen was abraded across the emery paper of grade 60 at a constant force of 10 N and at a constant speed of 0.32 m/s. Then an abraded distance of 40 m was reached, the test specimen was automatically elevated from the DIN abrader emery paper. The DIN volume loss or abrasion loss of the rubber nanocomposites was calculated using Equation (2). Minimum of 5 specimens per sample was tested and recorded and then the average value was taken as the abrasion loss for each sample.

$$Abrasionloss(mm^3) = (\Delta m \times S_0) \,/\, (\rho \times S) \tag{5}$$

where Δm is a mass loss (mg); ρ is a density (mg/mm^3); S_0 is a value of nominal abrasive power (200 mg); S is an average abrasive power (mg).

2.4 Swelling Measurements

Swelling test according to ASTM D471 was performed on 25 x 25 x 2 mm^3 cut a sample from the vulcanised sheet by the immersion method and were dried for 24 hours in a vacuum desiccator. The corners of the specimen were slightly curved to obtain uniform absorption. The thickness of the test samples was measured using a digital Vernier calliper with an accuracy of ±0.01 mm. The initial weight of the specimens was measured and was completely immersed in aromatic (benzene, toluene, xylene and mesitylene), aliphatic (n-pentane, n-hexane, n-heptane and n-octane) and chlorinated hydrocarbons (dichloromethane, chloroform, and carbon tetrachloride) in glass diffusion bottles. At regular intervals, the samples were removed from the glass diffusion bottles and clean the surface of the samples using tissue paper and weighed on a highly sensitive electronic balance with ±0.001 g. samples were then placed back into the glass diffusion bottles. The process was repeated until equilibrium swelling was obtained. The mole cent uptake Q_t for solvent was determined using the formula.

$$Q_t(mol\%) = \frac{(M_t - M_0)/MW}{M_0} X100 \tag{6}$$

where M_t is the mass of the specimen after time 72 h of immersion, M_0 is the initial mass of the specimen and MW is the molecular weight of the solvent.

2.4.1 Compression Set Measurements

Compression set test was carried out according to ASTM D395 [40]. The test sample is placed in the middle of the rectangular plates of the compression device by the spacers arranged on each side of it, allowing adequate clearance for bulging of the rubber when a compressive load is applied. The bolts tightened; therefore they are drawn

together uniformly until in contact with the spacers. The percentage of compression working is 25% of its original thickness. Then the assembled device was placed at 23 °C, 70 °C, and 100 °C for 1 day and 23 °C for 2 and 3 days in an air circulating oven. After completion, compression device is taken from the air circulating oven and then the test specimen removed instantaneously and allowable to cool for 30 min. The final thickness is measured by an electronic digital Vernier calliper with 0.01 mm accuracy. The compression set was determined using formula

$$\text{Percentage of compression set, } C\% = \frac{t_0 - t_1}{t_0 - t_s} X100 \qquad (7)$$

where t_0 is the original thickness of the specimen, t_1 is the specimen thickness after removed from the compression device and t_s is the spacer bar thickness which is used.

2.4.2 Field emission scanning electron microscopy (FESEM)

Field emission-scanning electron microscopy (Hitachi S4160, Japan) were employed to study the morphology of the fractured surface obtained from the tensile test under an acceleration voltage of 3 kV, coated with a gold layer.

3 Results and Discussions

3.1 Rheometric Characteristics

For filled compounds, type and content of filler affect the cure characteristics [41]. Table 2 shows the rheometric characteristics of EPDM/SBR-nanoclay vulcanizates with a different crosslinking system under investigation. The rheometric characteristics such as minimum torque, maximum torque, delta torque (difference between maximum torque and minimum torque), scorch time, optimum cure time and cure rate index were studied. Minimum torque is directly related to the viscosity of the compounds at the test temperature. The minimum torque can be calculated as the measure of the viscosity of the masticated rubber. Whenever there is excessive mastication, the viscosity registers a sharp decrease. The nanoclay loaded EPDM/SBR vulcanizates show that minimum torque, maximum torque and delta torque (ΔM) increases with increasing content of nanoclay for all of the crosslinking system. Maximum torque value can be related to as the measure of stock modulus [42]. Peroxide cured compound shows higher minimum torque, maximum torque, and delta torque value than the other cured compounds. The delta torque is an indirect indication of the degree of crosslinking of the rubber vulcanizates [43]. This shows that ΔM increase continuously with increasing content of nanoclay for different curing system. This may be due to the ethylene and propylene monomers present

Table 2 Rheometric characteristics of the EPDM/SBR/NC compounds

Sample code	Min. torque (dN m)	Max. torque (dN m)	Torque difference (dN m)	Scorch time (min.)	Optimum cure time (min.)	Cure rate index (min^{-1})
S_0	1.01	6.30	5.29	4.18	7.17	33.44
$S_{2.5}$	1.06	6.52	5.46	1.92	4.30	42.02
S_5	1.13	6.71	5.58	1.87	4.09	45.05
$S_{7.5}$	1.21	6.82	5.61	1.8	3.97	46.08
S_{10}	1.28	6.98	5.70	1.64	3.89	44.44
P_0	1.22	7.46	6.24	5.14	11.94	14.71
$P_{2.5}$	1.35	7.93	6.58	2.73	8.42	17.57
P_5	1.46	8.13	6.67	2.67	8.29	17.79
$P_{7.5}$	1.53	8.52	6.99	2.59	8.19	17.86
P_{10}	1.61	9.15	7.54	2.50	8.13	17.76
M_0	1.08	7.24	6.16	4.62	8.89	23.42
$M_{2.5}$	1.18	8.45	7.27	1.97	5.46	28.65
M_5	1.22	9.12	7.90	1.91	5.33	29.24
$M_{7.5}$	1.27	9.31	8.04	1.86	5.26	29.41
M_{10}	1.42	9.55	8.13	1.79	5.17	29.59

in EPDM [44]. The scorch and optimum cure time value decreases but cure rate index increases with increasing content of nanoclay. The optimum cure time and scorch time were reduced in the nanoclay loaded nanocomposites than the base rubber. Scorch time is a measure of the premature vulcanisation of the nanocomposites. These results can be due to the good interactions and interfacial adhesion between the nanoclay and the rubber matrix. Hasty vulcanising reaction in the nanocomposites was activated by the large surface area of the nanoclay. Amongst the different crosslinking systems for given nanoclay loading, the scorch safety was highest for peroxide system and lowest for sulphur cured system. The optimum cure time has been found to be highest for peroxide cured systems compared with sulphur and mixed systems for a given nanoclay loading. A high CRI value shows higher vulcanisation rate. This may be attributed to the nanoclay acts as an effective crosslinking agent for SBR/EPDM nanocomposites and it is leading a substantial increase in the rubber vulcanisation rate [44–46]. In fact, the amine groups existing in the nanosilicate structure, which originate from the organophilization of the nanoclay, ease the curing reaction of neat rubber [53]. This result is due to the intercalation of the rubber chains between the silicate layers, and therefore increasing the interlayer distance which eases the loading of EPDM/SBR chains into the silicate layers.

3.2 Mechanical Properties

The additions of fillers in the matrix enhance the tensile strength, tensile modulus, hardness and tear strength of the composite. The reinforcement's effect in the polymer materials is directly related to the interphase properties and depends on the nature of the specific interactions between the polymer matrix and reinforcing fillers [47]. The incorporation of filler into the polymer materials imparts many useful properties to the filler filled composite materials. The properties mostly depend on the dispersion condition of filler particles such as particle size, surface area, surface activity, aggregate structure and rubber-filler interactions [48]. Optimum reinforcing control can be achieved by the advantage of filler is better dispersed in the rubber matrix. The chemical or physical interaction between the filler and the rubber is an additional important aspect in the reinforcing effect [49]. The interaction between reinforcing fillers and rubber matrix has an important effect on the properties of rubber composite. A rubber-rubber interaction primarily occurs when rubber blends are used in composites and are not considered as important to filler-filler and filler-rubber interactions. Filler-filler interaction is explained by the attraction of filler to filler and the ability to form a network whilst filler-rubber interactions are explained by the compatibility of the filler with the rubber. Filler-filler interactions are a most important mechanism in reinforcement, particularly at high filler loading. These interactions depend on chemical interactions between the filler particle surfaces such as filler-filler and filler-rubber, physical interactions such as Vander Waals forces and hydrogen bonding, filler volume fraction and morphology of the filler network.

The interaction between the clay platelets having a large surface area as well as polymer chains enables stress transfer to the reinforcement phase, causing improved tensile properties. The stress-strain curves for EPDM/SBR vulcanizates filled with nanoclay loading are shown in Fig. 1. Tensile properties (tensile strength, elongation at break and 100% modulus) are obtained from the stress-strain curve.

The tensile strength of unaged and thermally aged sulphur, peroxide and mixed system cured EPDM/SBR blends as a function of nanoclay loading as shown in Fig. 2. The tensile strength of unaged nanocomposites increases with increase in nanoclay content up to 7.5 phr and then decreases for all the three different curing system. This is due to the crosslink density as shown in Table 4. The crosslinking efficiency of the nanoclay filled EPDM/SBR blends is measured in terms of crosslink density. The increase of tensile strength is directly related to the amount of dispersion of the nanoclay within the rubber matrix. The generally increased filler of the nanocomposites may be attributed to the dispersed structure of nanoclay at the nano-level, the planar orientation and the high aspect ratio of the silicate layers [54]. The filler is also related to the anisotropy property and high aspect ratio of nanoclay fillers, which act as short fibres with nano-scale architecture. Nanoclay with the high aspect ratio is more efficient in restricting the rubber chains and also in resisting the cracks development than spherical fillers [45]. All the types of cured thermally aged samples show a significant increase in the tensile strength. This is due to the creation of extra crosslinks during thermal ageing as shown by the crosslinking density values in Table 4. Samples are generally cured in the industry only to 90% of their maximum torque [50]. The grant of remaining 10% is usually kept to provide accommodations for the introduction of crosslinks in the matrix during service. Sulphur cured system exhibit the best tensile strength before and after ageing compared to peroxide and mixed system. A schematic representation of different crosslinks (sulphur, DCP and mixed system) formed between the macromolecular chains through different vulcanisation method is presented in Fig. 3. The chemical bonding between EPDM and SBR was formed via sulphur, peroxide and mixed system crosslinking between saturated and unsaturated rubbers as shown in Fig. 4. For unfilled blend systems (S_0, P_0, and M_0), the peroxide cured systems have rigid C—C bonds, which can be broken without difficulty under an applied stress, but in other systems (sulphur

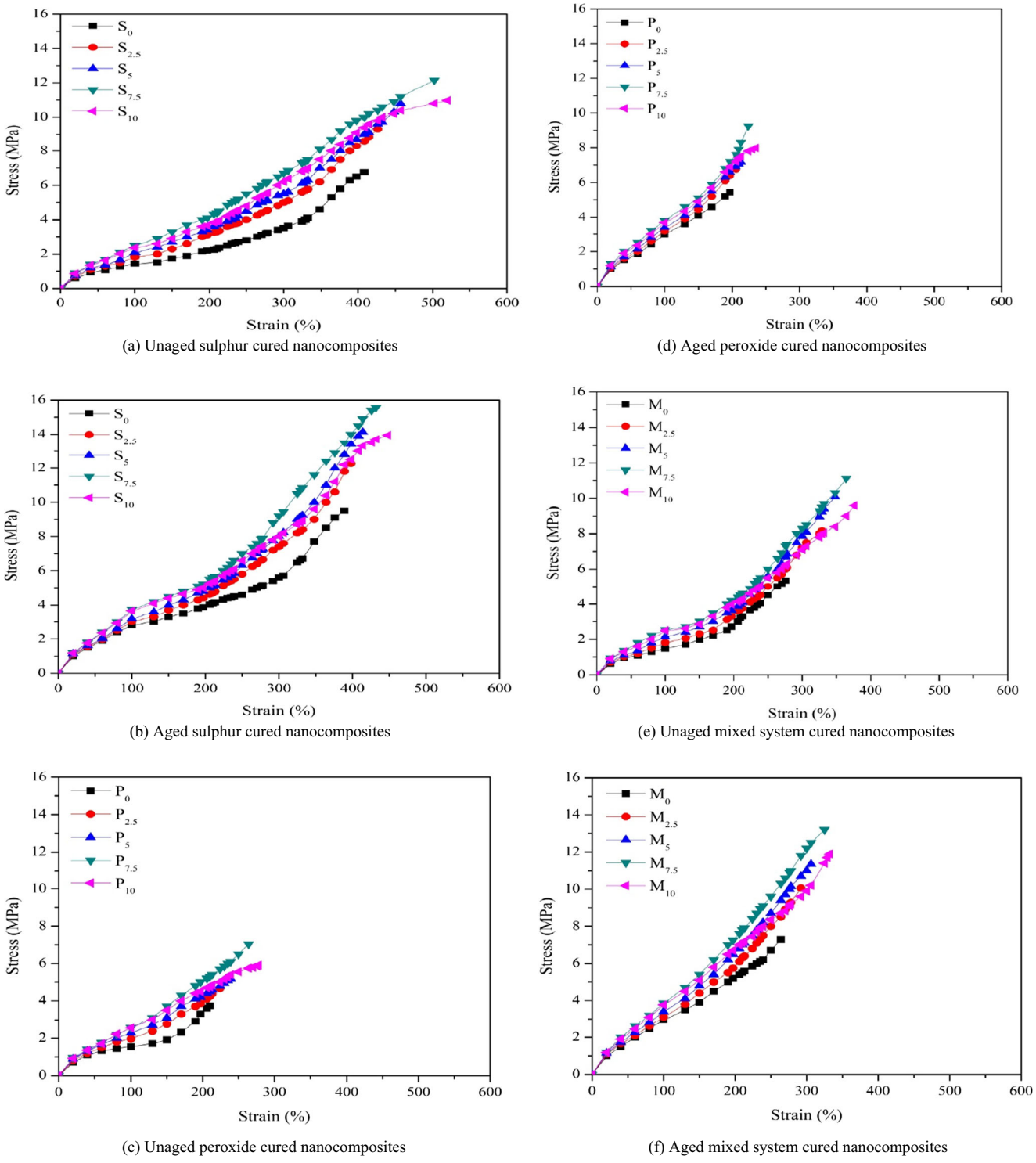

(a) Unaged sulphur cured nanocomposites

(d) Aged peroxide cured nanocomposites

(b) Aged sulphur cured nanocomposites

(e) Unaged mixed system cured nanocomposites

(c) Unaged peroxide cured nanocomposites

(f) Aged mixed system cured nanocomposites

Fig. 1 The stress-strain curves of unaged and thermally aged sulphur, peroxide and mixed system cured EPDM/SBR/NC rubber blends

and mixed), the flexible S—S and C—S bonds exist and they have need of more stress to break the bonds. The proposed interactions of nanoclay filled EPDM/SBR blends nanocomposite via sulphur and peroxide crosslinking as illustrated in Fig. 5. Addition of nanoclay improved the dispersion of filler in EPDM and SBR blends because it provides chemical bonds between fillers and polymers.

The effect of nanoclay loading on the elongation at break of unaged and thermally aged sulphur, peroxide and mixed system cured EPDM/SBR rubber blends as shown

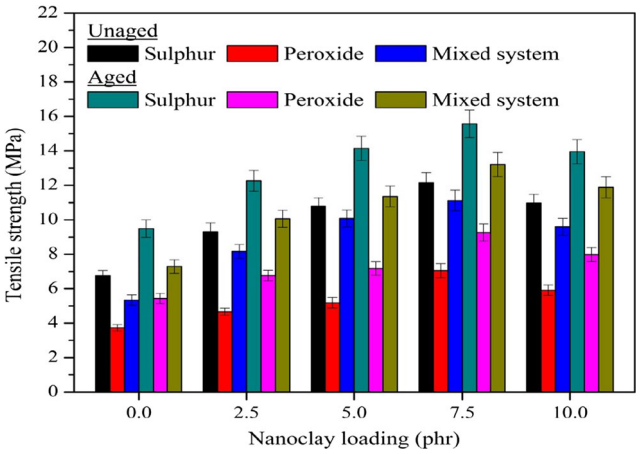

Fig. 2 Tensile strength of EPDM/SBR nanocomposites

in Fig. 6. The elongation at break of unaged and thermally aged EPDM/SBR rubber blends increases with increase in the content of nanoclay for all the three different curing systems. The elongation at break decreases for thermally aged samples compare to that of corresponding unaged samples. Sulphur cured system exhibit the best elongation at break of unaged samples compared to peroxide and mixed system. The peroxide cured system exhibits the lower elongation at break due to the C—C bonds between the macromolecular chains. The crosslink density increase for thermally aged samples, the mobility of the rubber chains

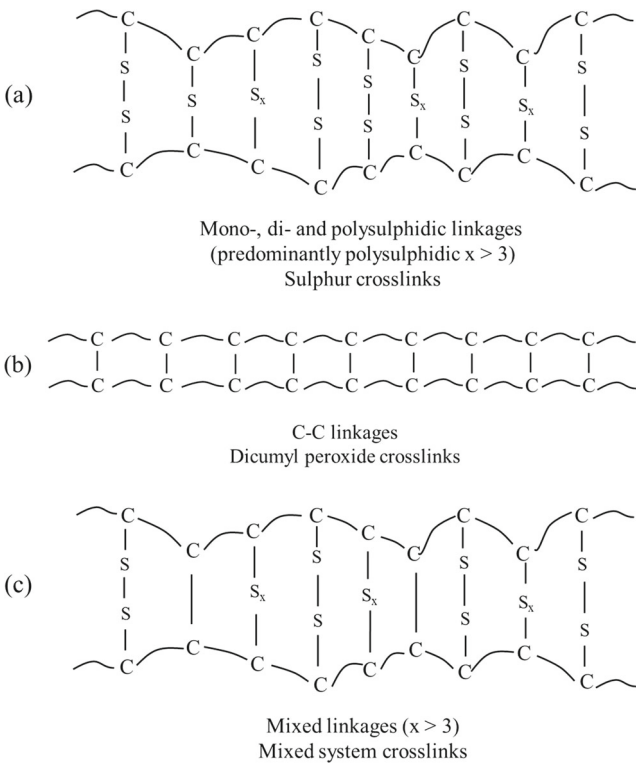

Fig. 3 Schematic representation of the nature of the crosslinks

is reduced. Incorporation of nanoclay into the EPDM/SBR matrix was found to improve elongation at break of nanocomposites. Generally, at favourable matrix/nanoclay interactions and relatively low nanoclay content, both tensile strength and elongation at break increased [51–54].

The effect of nanoclay loading on the 100% modulus of unaged and thermally aged sulphur, peroxide and mixed system cured EPDM/SBR/NC rubber blends as shown in Table 3. The 100% modulus of unaged and thermally aged EPDM/SBR rubber blends increased rapidly with increasing the concentration of nanoclay (2.5-7.5 phr) and with further increase in the addition of nanoclay, the 100% modulus decreases. The 100% modulus increase in thermally aged samples compare to the corresponding unaged samples. This is because of crosslink network increase due to the post-curing during thermally ageing treatment. Peroxide cured system exhibit the best 100% modulus unaged and thermally aged compared to sulphur and mixed system. The modulus is the direct measurement of the reinforcing effect of the nanofillers. The results of M_{100f}/M_{100u} are represented in Table 3. The measure of the reinforcement effect on the nanoclay filler is the ratio of 100% modulus of nanoclay filled nanocomposites (M_{100f}) to that of unfilled EPDM/SBR nanocomposites (M_{100u}) [55]. This ratio increased rapidly with increasing content of nanoclay (2.5 to 7.5 phr) and then decreases. The reinforcing effect is decreased for EPDM/SBR nanocomposites with higher nanoclay concentration owing to the poor dispersion of nanoclay [56].

The effect of nanoclay loading on the hardness of unaged and thermally aged sulphur, peroxide and mixed system cured EPDM/SBR rubber blends as shown in Fig. 7. The hardness of unaged and thermally aged EPDM/SBR rubber blends increases with increase in the content of nanoclay for all different curing systems. This could be attributed to the large surface area of nanoclay dispersed at nano-level and the largest aspect ratio of silicate layers, which consequences the increased silicate layer networking [45]. Higher crosslink density is responsible for higher hardness. The hardness of thermally aged samples increases compared to the corresponding unaged samples due to the crosslink density being increased. Crosslink density increases, the softer matrix turns into harder one. Peroxide cured system exhibits the best hardness of unaged and aged samples compared to sulphur and mixed system.

The effect of nanoclay loading on the tear strength of unaged and thermally aged sulphur, peroxide and mixed system cured EPDM/SBR rubber blends as shown in Fig. 8. The tear strength of unaged and thermally aged EPDM/SBR rubber blends increases with increase in the content of nanoclay for all different curing systems. Sulphur cured system exhibit the best tear strength of unaged and aged samples compared to peroxide and mixed system. The

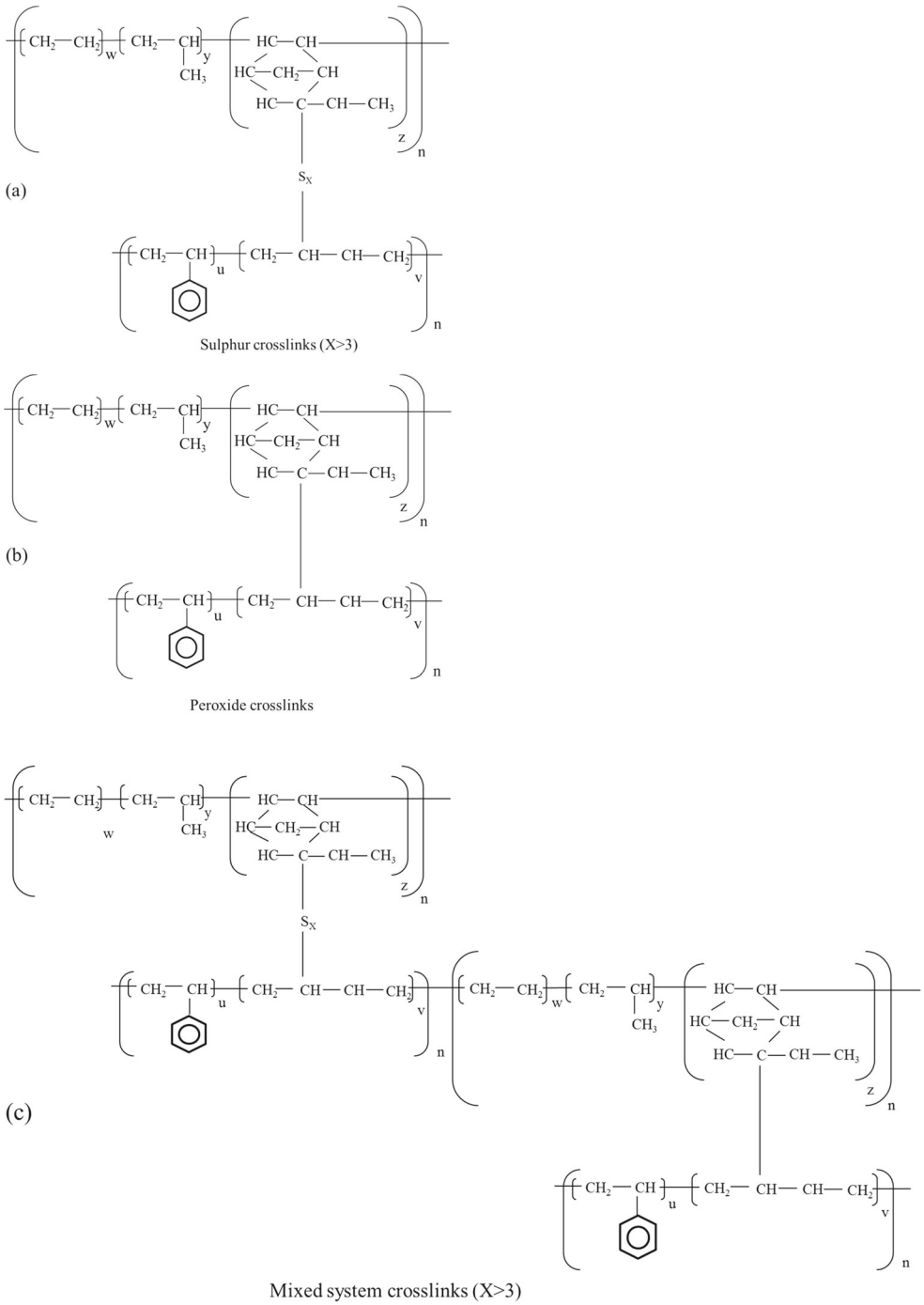

Fig. 4 The proposed interaction of EPDM/SBR blends with different cross-linkers

peroxide cured system exhibited lower tear strength due to the short and rigid C—C bonds.

3.3 Rebound Resilience

The effect of nanoclay loading on the rebound resilience of unaged and thermally aged sulphur, peroxide and mixed system cured EPDM/SBR rubber blends are seen in Table 3. The rebound resilience of unaged and aged nanocomposites decreases with an increase in nanoclay content for all the three different curing system. The decreasing tendency may be attributed to better rubber-filler interaction. As filler particles increases in the rubber matrix, the elasticity of the rubber chains is reduced, resulting in lower rebound resilience [59]. The surface activity is a major factor, showing the extent of rubber-filler interaction. The increase in the content of nanofillers in the rubber matrix, increases the hardness of the nanocomposites, whereas the rebound resilience tends to decrease [60]. The rebound resilience of the (S_{10}, P_{10}, and M_{10}) nanocomposites was 15%, 20%,

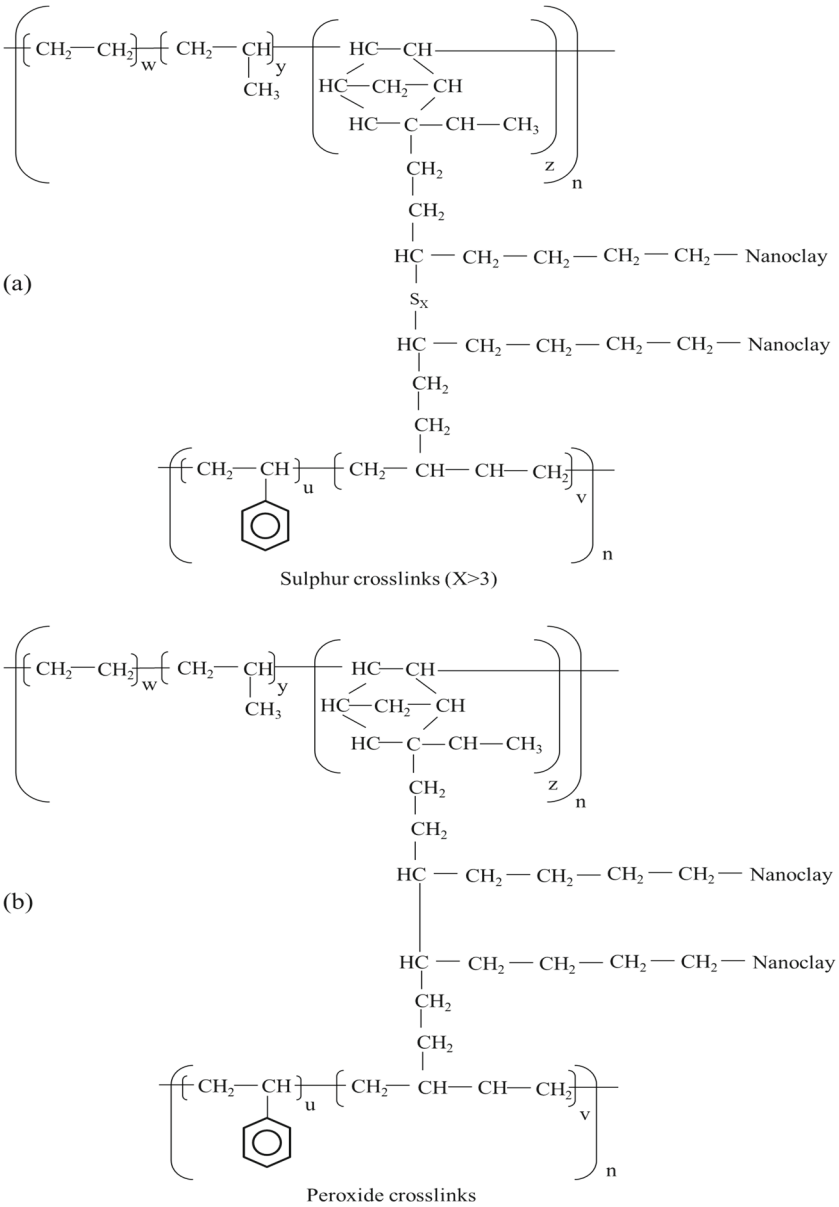

Fig. 5 The proposed interactions of nanoclay filled EPDM/SBR blends nanocomposite

and 14% lesser than their respective controls (S_0, P_0 and M_0). From the Table 3, sulphur cured nanocomposites shows the highest rebound resilience. Rebound resilience at different crosslinking systems follows the order sulphur >mixed >peroxide. The peroxide cured system exhibits lower rebound resilience due to the C—C bonds between the macromolecular chains.

3.4 Abrasion Resistance

Abrasion resistance of the nanoclay filled EPDM/SBR nanocomposites, expressed as an abrasion loss has been studied for sulphur, peroxide and mixed system cured blends, and is presented in Table 3. The abrasion resistance of nanocomposites increases with the increase in nanoclay content for all the three different curing system. At given nanoclay loading, the abrasion resistance of thermally aged nanocomposites is noticeably greater than those in unaged nanocomposites. Nanoclay as reinforcing filler, that interacts better with the rubber phase, as revealed by the higher reduction of abrasion loss in the nanocomposites. This improvement may be due to the better rubber-filler interfacial adhesion and greater surface area resulting in an enhanced abrasion resistance [61]. The peroxide cured system exhibits higher abrasion loss, sulphur cured system shows the lowest abrasion loss and the mixed system exhibited an intermediate behaviour. It is evident that the abrasion resistance of the $S_{2.5}$, S_5, $S_{7.5}$, and S_{10} of the sulphur cured nanoclay loaded nanocomposites was 31%, 44%, 54% and 59% higher than that of their respective

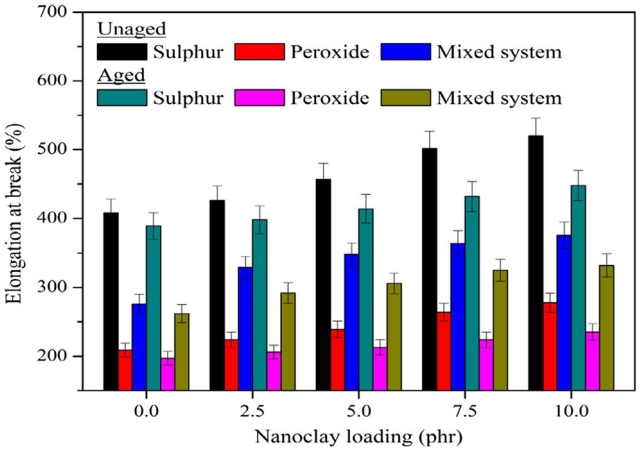

Fig. 6 Elongation at break of EPDM/SBR nanocomposites

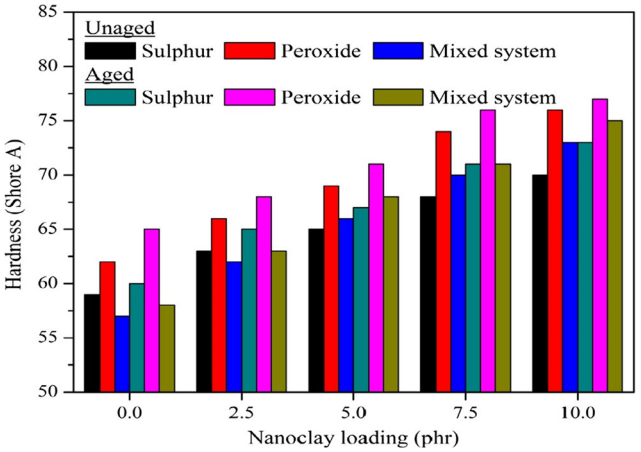

Fig. 7 Hardness of the EPDM/SBR nanocomposites

control S_0. Similarly, peroxide cured nanocomposites was 18%, 27%, 32% and 34% as well as mixed system cured nanocomposites was 18%, 29%, 36% and 43% higher than that of their respective control P_0 and M_0.

3.5 Swelling Study

Polymers are used in different applications particularly in barrier applications and are exposed to a variety of chemical environments during their lifetime. The swelling curves are expressed as mole cent uptake (Q_t) of the polymer versus square root of time ($t^{1/2}$) is plotted. The effects of nanoclay loading, crosslinking systems, nature of penetrants and temperature on mole cent uptake through EPDM/SBR nanocomposites were analysed. The swelling behaviour of nanocomposites depends on the types of filler, matrix, the reaction between solvent and matrix, temperature, etc.

3.5.1 Effect of Nanoclay

Figure 9 shows the mole cent uptake of benzene by different nanoclay loading crosslinked with sulphur at 30 °C. The uptake of benzene is reduced for the nanoclay filled composites compared to unfilled compounds. The graph clearly shows that the EPDM/SBR blend has the highest equilibrium uptake, and incorporation of nanoclay in the blends, the mole cent uptake regularly decrease. The swelling of the penetrant solvent depends on the free space available in the polymer matrix to accommodate the penetrant molecule. The incorporation of nanoclay reduced

Table 3 100% modulus, rebound resilience and abrasion loss of unaged and aged EPDM/SBR/NC rubber blends

Sample code	100% modulus (MPa)		M_{100f}/M_{100u}		Rebound resilience (%)		Abrasion loss (mm^3)	
	Unaged	Aged	Unaged	Aged	Unaged	Aged	Unaged	Aged
S_0	1.44	2.81	1	1	78	52	79.1	72.3
$S_{2.5}$	1.83	3.02	1.27	1.07	77	49	60.3	54.4
S_5	2.09	3.18	1.45	1.13	74	44	54.8	48.4
$S_{7.5}$	2.51	3.76	1.74	1.34	70	42	51.2	47.8
S_{10}	2.37	3.67	1.65	1.31	66	38	49.9	46.4
P_0	1.55	2.98	1	1	71	48	189.8	175.1
$P_{2.5}$	1.96	3.17	1.26	1.06	69	43	161.4	152.6
P_5	2.28	3.39	1.47	1.14	66	38	149.7	142.2
$P_{7.5}$	2.55	3.81	1.65	1.28	62	36	144.3	137.4
P_{10}	2.55	3.69	1.65	1.24	57	30	141.9	135.5
M_0	1.48	2.94	1	1	73	49	113.8	102.6
$M_{2.5}$	1.81	3.11	1.22	1.06	72	45	96.8	88.4
M_5	2.13	3.41	1.44	1.16	70	41	88.1	83.2
$M_{7.5}$	2.53	3.86	1.71	1.31	66	38	83.9	79.7
M_{10}	2.48	3.77	1.68	1.28	63	33	79.5	75.2

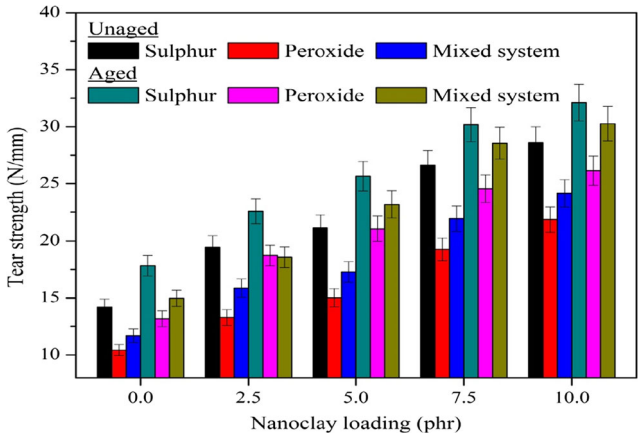

Fig. 8 Tear strength of the EPDM/SBR nanocomposites

the availability of these free spaces in the EPDM/SBR matrix, the restricted segmental mobility of EPDM/SBR matrix and creates the tortuous path for transport of penetrant molecules through the nanocomposites. The same trend is observed with aromatic, aliphatic and chlorinated hydrocarbons as shown in Table 4.

3.5.2 Effect of Crosslinking Systems

The mole cent uptake of 5 phr nanoclay filled EPDM/SBR nanocomposites crosslinked with sulphur, peroxide and mixed systems is seen in Figure 10. The penetrant used is toluene and the experiments conducted at 30 °C. The graph clearly shows that the sulphur cured nanocomposites absorbs the highest amount of solvent whilst the peroxide cured nanocomposites take up the lowest amount. The mixed system cure nanocomposites exhibited an intermediate behaviour. The difference in the uptake values of

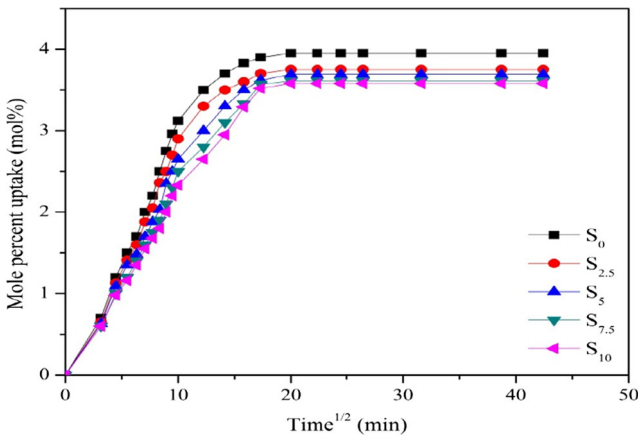

Fig. 9 Mole cent uptake of benzene by different nanoclay loading crosslinked with sulphur at 30 °C

Table 4 Mole cent uptake of aromatic, aliphatic and chlorinated penetrant of EPDM/SBR-NC composites at 30 °C

Sample code	Mole cent uptake (mol%) at 30 °C											
	Aromatic				Aliphatic				Chlorinated			
	Benzene	Toluene	Xylene	Mesitylene	n-pentane	n-hexane	n-heptane	n-octane	Dichloromethane	Chloroform	Carbon tetrachloride
S_0	3.95	3.57	3.46	3.03	2.42	2.34	2.28	2.24	5.42	4.56	2.26
$S_{2.5}$	3.75	3.32	2.78	2.52	2.14	2.09	2.06	2	4.77	4.25	2.05
S_5	3.69	3.27	2.55	2.31	2.08	1.98	1.94	1.91	4.65	4.1	1.98
$S_{7.5}$	3.61	3.11	2.47	2.22	1.97	1.92	1.87	1.82	4.45	4.02	1.88
S_{10}	3.58	3.08	2.44	2.15	1.95	1.87	1.82	1.78	4.39	3.91	1.83
P_0	2.58	2.27	2.07	2	1.95	1.9	1.84	1.81	3.47	3.36	2.24
$P_{2.5}$	2.41	2.16	2.02	1.91	1.72	1.7	1.68	1.65	3.28	3.13	1.86
P_5	2.37	2.09	1.99	1.89	1.64	1.6	1.54	1.5	3.16	2.81	1.75
$P_{7.5}$	2.29	2.01	1.84	1.85	1.58	1.54	1.48	1.45	2.95	2.77	1.7
P_{10}	2.24	1.97	1.81	1.81	1.55	1.49	1.46	1.38	2.91	2.71	1.65
M_0	2.85	2.48	2.41	2.35	2.32	2.26	2.18	2.14	3.8	3.42	2.29
$M_{2.5}$	2.71	2.39	2.28	2.23	2.21	2.14	2.05	2	3.63	3.21	2.04
M_5	2.66	2.36	2.19	2.17	2.08	2.02	1.97	1.94	3.54	3.1	1.92
$M_{7.5}$	2.58	2.28	2.06	2	1.97	1.9	1.86	1.8	3.47	3.02	1.81
M_{10}	2.52	2.25	2.04	1.94	1.83	1.8	1.79	1.72	3.44	2.97	1.74

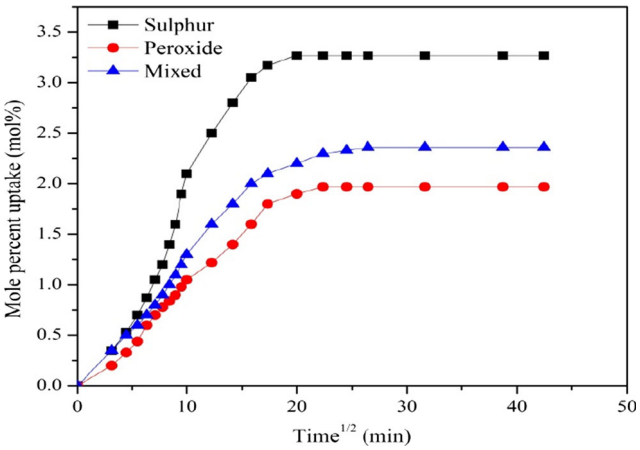

Fig. 10 Mole cent uptake of toluene by 5 phr nanoclay filled nanocomposites with different crosslinking systems at 30 °C

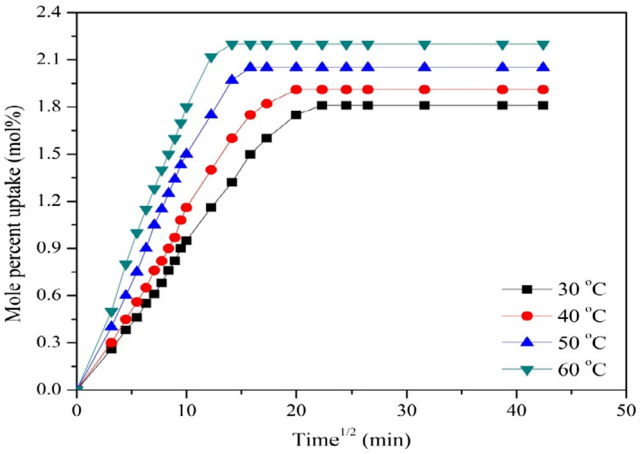

Fig. 12 Temperature dependence of the mixed system crossliked 7.5 phr nanoclay filled nanocomposites in carbon tetrachloride

nanocomposites with different crosslinking systems may possibly due to the formation of different types of crosslinks between rubber chains during vulcanisation [62, 63]. The same trend is observed with aromatic, aliphatic and chlorinated hydrocarbons as shown in Table 4.

3.5.3 Effect of Penetrant Size

The effect of penetrant size on the mole cent uptake of four aliphatic hydrocarbons through 7.5 phr nanoclay filled EPDM/SBR nanocomposites crosslinked with peroxide is seen in Fig. 11. It is clear from the figure that the trend is in the order: n-pentane >n-hexane >n-heptane >n-octane. The low molecular weight of the penetrant molecule shows the highest uptake but the high molecular weight of the solvent shows the lowest uptake. Generally, the solvent penetrant and molecular mass are inversely related. The same trend is observed with aromatic, aliphatic and chlorinated hydrocarbons as shown in Table 4.

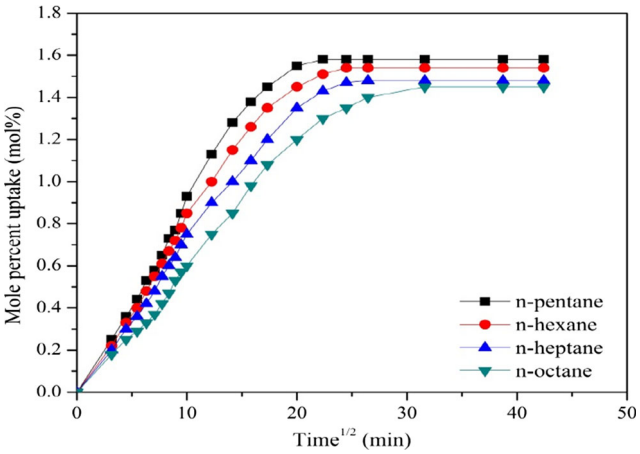

Fig. 11 Mole cent uptake of peroxide crosslinked 7.5 phr nanoclay filled nanocomposites

3.5.4 Effect of Temperature

The effect of temperature on the mole cent uptake of carbon tetrachloride through 7.5 phr nanoclay filled EPDM/SBR nanocomposites crosslinked with mixed systems is depicted in Fig. 12. As the temperature increased, the mole cent uptake also increased for all the nanocomposites. The thermal energy increased with increases in temperature and hence the free void volume in the polymer matrix, a molecular vibration of solvent molecules and flexibility of the polymer chains increased [64]. The mole cent uptake at 40 °C, 50 °C and, 60 °C are shown in Tables 5, 6 and 7.

3.6 Crosslinking Density

The crosslinking density is calculated from the swelling data. The molecular weight of the polymer between the crosslinks (M_c) plays an important role in the determination of crosslinking density. The estimated values of M_c for EPDM/SBR nanocomposites are tabulated in Table 8. Nanoclay filled composites have lower M_c values than unfilled EPDM/SBR nanocomposites. Molar mass between crosslinks (M_c) deceased with increasing nanoclay content. As the M_c values decreased, the available volume between adjacent crosslinks decreased. The crosslinking density values of EPDM/SBR nanocomposites are reported in Table 8. As the nanoclay content in the nanocomposites increased, the crosslinking density also increased. Higher crosslinking density provides higher tensile strength, tensile modulus, tear strength, hardness and abrasion resistance.

Table 5 Mole cent uptake of aromatic penetrant of EPDM/SBR-NC composites at 40 °C, 50 °C, and 60 °C

Sample code	Mole cent uptake (mol%)											
	Benzene			Toluene			Xylene			Mesitylene		
	40 °C	50 °C	60 °C	40 °C	50 °C	60 °C	40 °C	50 °C	60 °C	40 °C	50 °C	60 °C
S_0	4.06	4.2	4.31	3.72	3.9	4.03	3.54	3.62	3.78	3.26	3.45	3.6
$S_{2.5}$	3.89	4.04	4.16	3.48	3.66	3.95	2.96	3.54	3.65	2.91	3.24	3.42
S_5	3.82	3.97	4.05	3.41	3.54	3.66	2.81	3.49	3.57	2.84	3.13	3.33
$S_{7.5}$	3.78	3.88	3.99	3.36	3.46	3.55	2.75	3.41	3.49	2.79	2.98	3.21
S_{10}	3.81	3.91	4.03	3.39	3.5	3.6	2.79	3.46	3.53	2.82	3.08	3.29
P_0	2.67	2.8	2.94	2.34	2.5	2.59	2.13	2.35	2.48	2.11	2.29	2.4
$P_{2.5}$	2.55	2.69	2.8	2.27	2.38	2.48	2.08	2.26	2.41	2.07	2.2	2.3
P_5	2.49	2.6	2.9	2.2	2.32	2.41	2.02	2.2	2.35	2.01	2.12	2.23
$P_{7.5}$	2.44	2.54	2.63	2.13	2.23	2.35	1.96	2.09	2.22	1.93	2	2.1
P_{10}	2.46	2.56	2.75	2.15	2.26	2.39	2	2.14	2.31	1.96	2.06	2.17
M_0	3.16	3.35	3.48	2.61	2.82	2.9	2.83	3	3.06	2.52	2.71	2.83
$M_{2.5}$	3.02	3.18	3.29	2.54	2.74	2.79	2.46	2.74	2.96	2.39	2.56	2.74
M_5	2.95	3.07	3.16	2.46	2.7	2.75	2.35	2.65	2.89	2.31	2.47	2.65
$M_{7.5}$	2.88	2.97	3.09	2.39	2.6	2.66	2.25	2.5	2.7	2.24	2.33	2.51
M_{10}	2.92	3.02	3.13	2.41	2.66	2.71	2.29	2.58	2.78	2.38	2.4	2.58

Table 6 Mole cent uptake of aliphatic penetrant of EPDM/SBR-NC composites at 40 °C, 50 °C, and 60 °C

Sample code	Mole cent uptake (mol%)											
	n-pentane			n-hexane			n-heptane			n-octane		
	40 °C	50 °C	60 °C	40 °C	50 °C	60 °C	40 °C	50 °C	60 °C	40 °C	50 °C	60 °C
S_0	2.59	2.72	2.85	2.5	2.63	2.74	2.36	2.5	2.63	2.31	2.46	2.53
$S_{2.5}$	2.31	2.59	2.68	2.39	2.48	2.61	2.19	2.41	2.56	2.23	2.34	2.46
S_5	2.17	2.45	2.57	2.23	2.35	2.5	2.1	2.28	2.46	2.11	2.24	2.4
$S_{7.5}$	2.08	2.33	2.46	2.17	2.25	2.41	2.02	2.15	2.31	2.04	2.12	2.28
S_{10}	2.12	2.42	2.51	2.21	2.33	2.46	2.05	2.21	2.38	2.07	2.18	2.35
P_0	2.14	2.29	2.41	2.06	2.2	2.32	2	2.12	2.29	1.92	2.05	2.2
$P_{2.5}$	2.02	2.2	2.29	2	2.1	2.22	1.94	2.03	2.2	1.85	1.96	2.1
P_5	1.94	2.12	2.22	1.94	2.02	2.11	1.88	1.95	2.09	1.69	1.8	2.01
$P_{7.5}$	1.87	2	2.1	1.85	1.96	2.04	1.83	1.9	2	1.57	1.66	1.91
P_{10}	1.91	2.07	2.18	1.88	1.99	2.09	1.85	1.92	2.05	1.62	1.72	1.97
M_0	2.43	2.54	2.61	2.38	2.49	2.61	2.27	2.35	2.48	2.26	2.39	2.45
$M_{2.5}$	2.37	2.46	2.55	2.26	2.4	2.5	2.1	2.22	2.36	2.14	2.3	2.34
M_5	2.3	2.35	2.48	2.15	2.3	2.38	2.02	2.14	2.29	2.07	2.22	2.26
$M_{7.5}$	2.21	2.28	2.39	2.03	2.16	2.21	1.95	2.04	2.15	1.94	2.1	2.14
M_{10}	2.23	2.31	2.45	2.08	2.23	2.29	1.98	2.08	2.21	1.98	2.15	2.2

Table 7 Mole cent uptake of chlorinated penetrant of EPDM/SBR-NC composites at 40 °C, 50 °C, and 60 °C

Sample code	Mole cent uptake (mol%)								
	Dichloromethane			Chloroform			Carbon tetrachloride		
	40 °C	50 °C	60 °C	40 °C	50 °C	60 °C	40 °C	50 °C	60 °C
S_0	5.63	5.74	5.89	4.8	4.91	5.07	2.38	2.54	2.71
$S_{2.5}$	4.96	5.12	5.28	4.67	4.78	4.91	2.22	2.39	2.58
S_5	4.84	4.98	5.13	4.4	4.56	4.8	2.09	2.22	2.41
$S_{7.5}$	4.67	4.85	5	4.28	4.45	4.68	2	2.08	2.23
S_{10}	4.73	4.91	5.05	4.32	4.51	4.73	2.07	2.14	2.29
P_0	3.61	3.74	3.85	3.57	3.7	3.82	2.31	2.46	2.6
$P_{2.5}$	3.44	3.62	3.76	3.38	3.54	3.62	2.14	2.29	2.42
P_5	3.29	3.47	3.6	3.11	3.32	3.48	1.99	2.13	2.31
$P_{7.5}$	3.08	3.21	3.47	2.98	3.14	3.32	1.84	2.02	2.16
P_{10}	3.15	3.28	3.54	3.05	3.22	3.36	1.86	2.05	2.21
M_0	4.05	4.16	4.3	3.8	4.11	4.32	2.35	2.5	2.65
$M_{2.5}$	3.86	4	4.21	3.62	3.98	4.19	2.19	2.34	2.51
M_5	3.72	3.85	4.08	3.49	3.72	3.99	2.04	2.16	2.37
$M_{7.5}$	3.6	3.75	3.95	3.21	3.45	3.66	1.91	2.05	2.2
M_{10}	3.65	3.79	4	3.25	3.54	3.75	1.96	2.09	2.25

3.7 Compression Set Properties

To determine the effect of nanoclay loading on the compression set behaviour of EPDM/SBR compounds, the compression set test was carried out at different conditions (at 23 °C for 1 day, 2 days, and 3 days, and at 70 °C and 100 °C for 1 day). Compression set is a measure of the rubbers ability to retain their elastic property after a prolonged compression at a constant strain under the specified condition, and it is a permanent set of rubber compounds [57, 58]. Table 8 represents the different crosslinking systems on the compression set for EPDM/SBR compounds filled with nanoclay loading under the conditions of 23 °C for 1 day. The compression set of the compound increases with increase in nanoclay loading. In the case of unfilled nanoclay compounds, the compression set is low, whilst an increase in the nanoclay loading, the compression set increases. This is because when the nanoclay loading increases the crosslinking density increases. Therefore, induce stiffness in the nanoclay filled compounds. Hence, the crosslink density increases which resulting in high percentage of compression set. The sulphur cured nanocomposite shows highest compression set. Compression set at different crosslinking systems follows the order sulphur >mixed >peroxide. A similar trend followed in compression set test at 23 °C (for 2 and 3 days) and at 70 °C and 100 °C (for 1 day). As the hours and temperature increases, the compression set also increases. The temperature is majorly effect the compression set and highly reduces the retainable properties. The lower compression set shows the better the retainable elastic properties. The compression set is lower, the better the material for use.

3.8 Morphology of Blend

Morphology is a most important factor of rubber blends, which determine the degree to which the blends are compatible. The phase arrangement of the rubber blend is influenced by numerous factors, comprising the surface characteristics, blend ratio, the viscosity of each constituent and compounding process. The major factors that determine the ultimate morphology of the mixtures is their composition. The FESEM images of the tensile fractured surface of the nanoclay filled EPDM/SBR rubber blends as shown in Fig. 13. Figure 13a, b, Fig. 10c, d and Fig. 13e, f shows the morphology with the incorporation of 5 and 7.5 phr of nanoclay filled sulphur, peroxide and mixed system cured rubber blends, respectively. The compounds ($S_{7.5}$) show highly rougher morphology, tortuous fractured surface and many tear line compared to the other compounds. The many tear line shows the more energy needed to break the specimens. This is because of the good interactions between the nanoclay layers and EPDM/SBR matrix. The nanoclay were uniformly dispersed in the matrix alters the crack lines along their length depending on the orientation of nanoclay layers. This leads to more resistance for crack propagation and hence better tensile strength.

Table 8 Crosslinking density and compression set of the EPDM/SBR nanocomposites

Sample code	Molar mass between crosslinks, M_c, (g/mol)		Crosslinking density (X 10^{-4} g mol/cc)		Compression set (%)				
	Unaged	Aged	Unaged	Aged	For 1 day at 23 °C	For 2 days at 23 °C	For 3 days at 23 °C	For 1 day at 70 °C	For 1 day at 100 °C
S_0	5449	4294	0.92	1.16	4.1	9.74	13.14	21.67	25.23
$S_{2.5}$	4895	3295	1.02	1.52	6.03	10.43	15.36	22.53	26.55
S_5	4820	2831	1.04	1.77	6.38	10.94	16.63	23.03	27.68
$S_{7.5}$	4484	2762	1.12	1.81	6.72	11.52	17.97	23.76	28.05
S_{10}	4445	2669	1.12	1.87	6.98	12.16	18.87	23.98	28.73
P_0	2628	2256	1.9	2.22	1.97	4.63	6.18	7.56	8.29
$P_{2.5}$	2457	2138	2.04	2.34	2.92	5.04	7.84	8.94	9.51
P_5	2350	2055	2.13	2.43	3.12	5.67	8.66	9.57	9.89
$P_{7.5}$	2232	2004	2.24	2.5	3.27	5.88	9.07	10.32	10.46
P_{10}	2184	1971	2.29	2.54	3.35	6.18	9.39	10.67	11.23
M_0	3120	2975	1.6	1.68	2.89	6.85	9.12	10.78	11.38
$M_{2.5}$	2978	2780	1.68	1.8	4.07	7.92	11.33	11.92	14.28
M_5	2940	2667	1.7	1.87	4.34	8.39	11.96	12.5	15.42
$M_{7.5}$	2810	2618	1.78	1.91	4.86	8.74	13.23	14.94	17.07
M_{10}	2773	2571	1.8	1.94	5.17	9.44	13.93	15.38	20.24

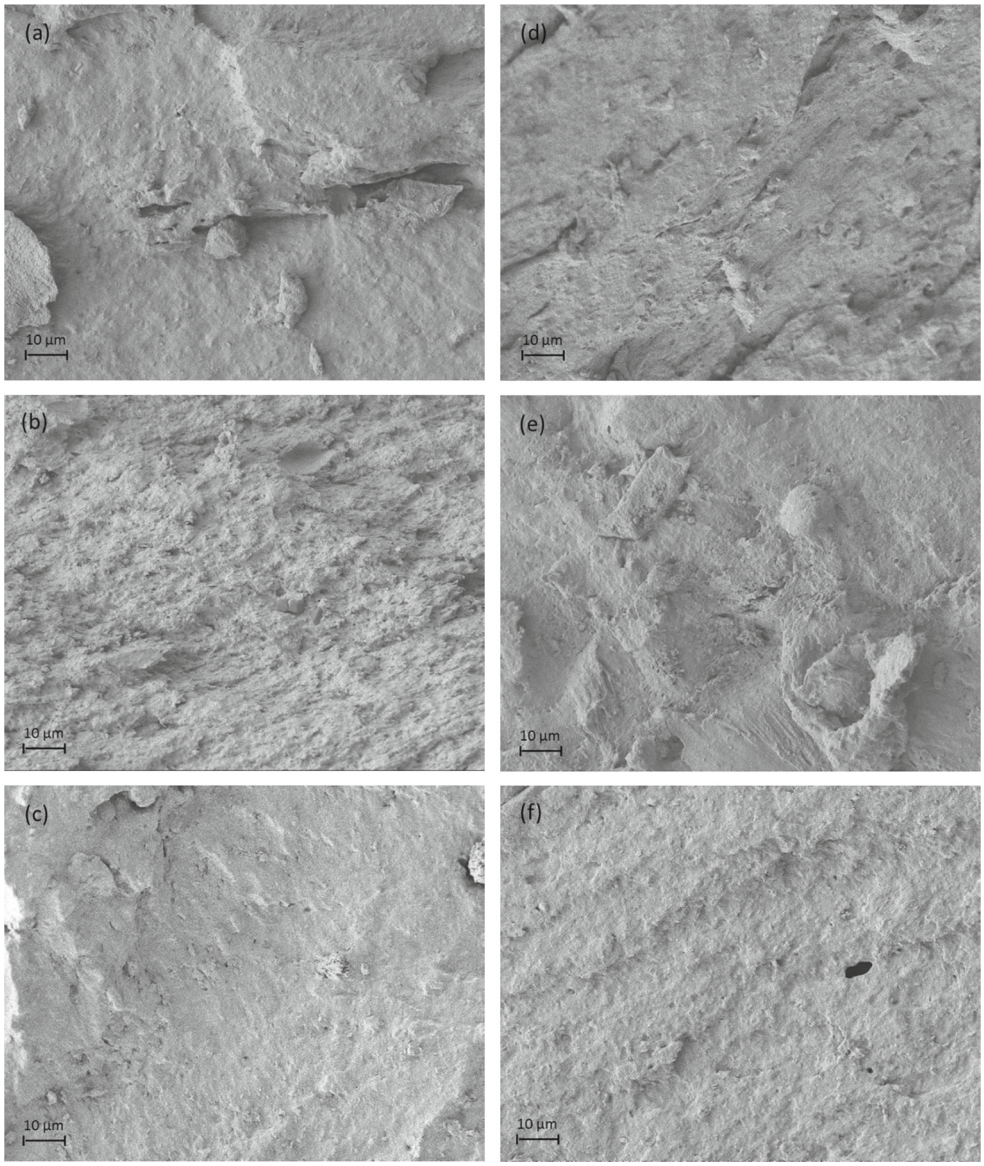

Fig. 13 The tensile fractured surfaces with magnification X = 1000 of nanoclay filled EPDM/SBR blends **a** S_5, **b** $S_{7.5}$, **c** P_5, **d** $P_{7.5}$, **e** M_5 and **f** $M_{7.5}$

4 Conclusions

In this work EPDM/SBR/Cloisite 30B nanocomposites were prepared by two roll mixing mill. Cure characteristics, tensile strength, 100% modulus, elongation at break, hardness, tear strength, rebound resilience, abrasion resistance, swelling resistance and compression set were conducted on EPDM/SBR rubber blends unaged and thermally aged with reference to the effects of nanoclay and crosslinking systems. The following conclusions were derived from the experimental results:

(1) Minimum torque, maximum torque and delta torque and cure rate index increases but scorch and optimum cure time values decrease with increasing content of nanoclay for all the three different curing system. The cure characteristics results reveal that nanoclay acted as an accelerating, crosslinking and reinforcing agent for EPDM/SBR chains. The increase in delta torque value was attained for the EPDM/SBR/nanoclay nanocomposites, showing a higher number of crosslinks formed. Peroxide cured compound shows higher minimum torque, maximum torque, and delta torque value than the other cured compounds.

(2) From attained effects, it was observed that strong interactions between EPDM/SBR-nanoclay caused in significantly improved rheological and mechanical properties.

(3) Tensile strength and 100% modulus of EPDM/SBR blend increases with increasing content of nanoclay up to 7.5 phr and then decreases.

(4) The sulphur cured systems exhibit increase in elongation at break of unaged nanocomposites with an increase in nanoclay content.
(5) Peroxide cured system on the hardness of aged rubber blends and sulphur cured system on the tear strength of aged rubber blends increases with increasing content of nanoclay.
(6) The incorporation of nanoclay into the EPDM/SBR was found to enhance tensile strength, 100% modulus, elongation at break, hardness, and tear strength.
(7) The peroxide cured nanocomposites shows lowest compression set and good swelling resistance properties. The penetrant uptake follows the order chlorinated >aliphatic >aromatic hydrocarbons for an EPDM/SBR nanocomposites. As the temperature increases, mole cent uptake increased thus, swelling resistance decreased.
(8) As the setup temperature and setup hours increased, compression set also increases. The compression set is lower, the better the material for use.
(9) It can be concluded that nanocomposites containing sulphur cured system give better overall mechanical properties and nanocomposites containing peroxide cured system give better compression and swelling resistance properties. The effects of this work show that the use of nanoclay as the reinforcing agent to the EPDM/SBR results in enhanced properties for prospective use in wide range of applications.

References

1. Giannelis EP, Krishnamorti R, Manias E (1999) Polymer-silicate nanocomposites: model systems for confined polymers and polymer brushes. Polym Confined Environ 138:107–147
2. Fukushima Y, Inagaki S (1987) Synthesis of an intercalated compound of montmorillonite and 6-polyamide. J Incl Phenom 5:473–482
3. Burnside SD, Giannelis EP (1995) Synthesis and properties of new poly (dimethylsiloxane) nanocomposites. Chem Mater 7:1597–1600
4. Mehrotra V, Giannelis EP (1990) Conducting molecular multilayers: intercalation of conjugated polymers in layered media. Mater Res Soc Symp Proc 171:39–44
5. Vaia RA, Jandt KD, Kramer EJ, Giannelis EP (1995) Kinetics of Polymer Melt Intercalation. Macromolecules 28:8080–8085
6. Wang Z, Pinnavaia TJ (1998) Nanolayer reinforcement of elastomeric polyurethane. Chem Mater 10:3769–3771
7. Lebaron PC, Wang Z, Pinnavaia TJ (1999) Polymer-layered silicate nanocomposites: an overview. Appl Clay Sci 15:11–29
8. Koo CM, Kim SO, Chung IJ (2003) Study on morphology evolution, orientational behavior, and anisotropic phase formation of highly filled polymer-layered silicate nanocomposites. Macromolecules 36:2748–2757
9. Kojima Y, Usuki A, Kawasumi M, Okada A, Fukushima Y, Kurauchi T, Kamigaito OJ (1993) Mechanical properties of nylon 6-clay hybrid. J Mater Res 8:1185–1189
10. Vaia RA, Vasudevan S, Krawiec W, Scanlon L, Lawrence G, Ginnelix EP (1995) New polymer electrolyte nanocomposites: Melt intercalation of poly (ethylene oxide) in mica-type silicates. Adv Mater 7:154–156
11. Chang YW, Yang Y, Ryu S, Nah C (2002) Preparation and properties of EPDM/organomontmorillonite hybrid nanocomposites. Polym Int 51:319–324
12. Giannelis EP (1996) Polymer layered silicate nanocomposites. Adv Mater 8:29–35
13. Wang S, Hu Y, Wang Z, Yong T, Chen Z, Fan W (2003) Synthesis and characterization of polycarbonate/ABS/montmorillonite nanocomposites. Polym Degrad Stab 80:157–161
14. Li JX, Wu J, Chan C-M (2000) Thermoplastic nanocomposites. Polymer 41:6935–6937
15. Alexandre M, Dubois P (2000) Polymer-layered silicate nanocomposites: preparation, properties and uses of a new class of materials. Mater Sci Eng: R: Rep 28:1–63
16. Arroyo M, Lopez Manchado MA, Herrero B (2003) Organomontmorillonite as substitute of carbon black in natural rubber compounds. Polymer 44:2447–2453
17. Varhgese S, Karger-Kocsis J (2003) Natural rubber-based nanocomposites by latex compounding with layered silicates. Polymer 44:4921–4927
18. Lopez Manchado MA, Herrero B, Arroyo M (2003) Preparation and characterization of organoclay nanocomposites based on natural rubber. Polym Int 52:1070–1077
19. Sadhu S, Bhowmick AK (2003) Effect of Chain Length of Amine and Nature and Loading of Clay on Styrene-Butadiene Rubber-Clay Nanocomposites. Rubber Chem Technol 76:860–875
20. Sadhu S, Bhowmick AK (2004) Preparation and properties of styrene-butadiene rubber based nanocomposites: the influence of the structural and processing parameters. J Appl Polym Sci 92:698–709
21. Chang YW, Yang YC, Ryu S, Nah C (2002) Preparation and properties of EPDM organomontmorillonite hybrid nanocomposites. Polym Int 51:319–324
22. Franta I (1989) Elastomers and Rubber Compounding Materials: Manufacture, Properties and Applications. Elsevier, Amsterdam
23. Morton M (1999) Rubber Technology. Springer Science Business Media, Dordrecht
24. Darrell M, Krishnamurthy J (2002) Strategies for Optimizing Polypropylene−Clay Nanocomposite Structure. Ind Eng Chem Res 41:6402–6408
25. Hambir S, Bulakh N, Jog JP (2002) Polypropylene/clay nanocomposites: effect of compatibilizer on the thermal, crystallization and dynamic mechanical behaviour. Polym Eng Sci 42:1800–1807
26. Lee KY, Goettler LA (2004) Structure-property relationships in polymer blend nanocomposites. Polym Eng Sci 44:1103–1111
27. Lal J (1970) Effect of Crosslink Structure on Properties of Natural Rubber. Rubber Chem Technol 43:664–686
28. Moore CG, Trego BR (1961) Structural characterization of vulcanizates. Part II. Use of triphenylphosphine to determine the structures of sulphur linkages in unaccelerated natural rubber–sulphur vulcanizate networks. J Appl Polym Sci 5:299–302
29. Kok CM, Yee VH (1986) The effects of crosslink density and crosslink type on the tensile and tear strengths of NR, SBR and EPDM gum vulcanizates. Eur Polym J 22:341–345
30. Chandra R, Mishra S, Parida TR (1995) Studies on dynamic behaviour and flow properties of HDPE/EPDM blends by torque rheometer. Polym Int 37:141–147
31. Durandish M, Alipour A (2013) Investigation into morphology, microstructure and properties of SBR/EPDM/ORGANO montmorillonite nanocomposites. Chin J Polym Sci 31:660–669

32. Muraleedharan Nair T, Kumaran MG, Unnikrishnan G (2004) Mechanical and aging properties of cross-linked ethylene propylene diene rubber / styrene butadiene rubber blends. J Appl Polym Sci 93:2606–2621
33. Oliveira MG, Soares BG (2001) The effect of the vulcanizing system on cure and mechanical properties of NBR/EPDM blends. Polym Polym Compos 9:459–467
34. Monfared A, Arani AJ (2015) Morphology and rheology of (styrene-butadiene rubber/acrylonitrile-butadiene rubber) blends filled with organoclay: The effect of nanoparticle localization. Appl Clay Sci 108:1–11
35. Mohan TP, Kuriakose Job, Kanny K (2011) Effect of nanoclay reinforcement on structure, thermal and mechanical properties of natural rubber–styrene butadine rubber (NR–SBR). J Ind Eng Chem 17:264–270
36. Jovanovic V, Jovanovic SS, Simendic JB, Markovic G, Cincovic MM (2013) Composites based on carbon black reinforced NBR/EPDM rubber blends. Compos: Part B 45:333–340
37. D15 ASTM (1958) Standard test method for rubber property-sample preparation for physical testing of rubber products. Annual Book of ASTM Standards, Philadelphia
38. Demirhan E, Kandemirli F, Kandemirli M (2007) The effects of furnace carbon blacks on the mechanical and the rheological properties of SBR1502 styrene butadiene rubber. Mater Des 28:1326–1329
39. Manoj KC, Kumari P, Rajesh C, Unnikrishnan G (2010) Aromatic liquid transport through filled EPDM/NBR blends. J Polym Res 17:1–9
40. 395 ASTMD (1955) Standard test method for rubber property-compression set of vulcanized rubber. Annual Book of ASTM Standards, Philadelphia
41. Coran Y (2003) Chemistry of the vulcanization and protection of elastomers: a review of the achievements. J Appl Polym Sci 87:24–30
42. Teh PL, Mohd Ishak ZA, Hashim AS, Karger-Kocsis J, Ishiaku US (2004) Effects of epoxidized natural rubber as a compatabilizer in melt compounded natural rubber-organoclay nanocomposites. Eur Polym J 40:2513–2521
43. Ismail H, Chia HH (1988) The effects of multifunctional additive and vulcanization systems on silica filled Epoxidized Natural Rubber compounds. Eur Polym J 34:1857–1863
44. Alipour A, Naderi G, Bakhshandeh GR, Shokoohi S (2011) Microstructure and Rheological Properties of NR/EPDM Nanocomposites: Effect of Composition. Iran Rubber Mag 62:26–34
45. Alipour A, Naderi G, Bakhshandeh GR, Vali H, Shokoohi S (2011) Elastomer nanocomposites based on NR/EPDM/organoclay: morphology and properties. Int Polym Process 26:48–55
46. Varghese S, Gatos KG, Apostolov AA, J Karger-Kocsis J (2004) Morphology and mechanical properties of layered silicate reinforced natural and polyurethane rubber blends produced by latex compounding. J Appl Polym Sci 92:543–551
47. Arrighi V, Gagliardi S, Higgins JS, Triolo A, Zanotti J-M Quasielastic neutron scattering as a probe of molecular motion in polymer-filler systems. E-MRS Spring Meeting 2002. Strasbourg (France). N-15
48. Persello J Designing nanostructured particular fillers for elastomers. Role of nanostructure and polymer filler interactions in rubber reinforcement. E-MRS Spring Meeting 2002. Strasbourg (France). N-8
49. Zaborski M, Donnet JB (2003) Activity of fillers in elastomer networks of different structure. Macromol Symp 194:87–100
50. Brown RP (1996) Physical Testing of Rubbers, 3rd edn. Chapman and Hall, London, p 74
51. Balachandran M, Bhagawan SS (2012) Mechanical, thermal and transport properties of nitrile rubber (NBR)-nanoclay composites. J Polym Res 19:9809
52. Munusamy Y, Ismail H, Mariatti M, Ratnam CT (2008) Ethylene vinyl acetate/natural rubber/organoclay nanocomposites: effect of sulphur and peroxide vulcanization. J Reinf Plast Compos 27:1925–1945
53. Zheng H, Zhang Y, Peng Z, Zhang Y (2004) Influence of clay modification on the structure and mechanical properties of EPDM/montmorillonite nanocomposites. Polym Test 23:217–223
54. Wu YP, Jia QX, Yu DS, Zhang LQ (2003) Structure and properties of nitrile rubber (NBR)-clay nanocomposites by co-coagulating NBR latex and clay aqueous suspension. J Appl Polym Sci 89:3855–3858
55. Kim JT, Oh TS, Lee DH (2003) Preparation and characteristics of nitrile rubber (NBR) nanocomposites based on organophilic layered clay. Polym Int 52:1058–1063
56. Pramanik M, Srivastava SK, Samantaray BK, Bhowmick AK (2002) Synthesis and characterization of organosoluble, thermoplastic elastomer/clay nanocomposites. J Polym Sci Part B: Polym Phys 40:2065–2072
57. Smith LP (1993) The language of rubber. Butterworth, Heinemann, London
58. Othman AB (2001) Property profile of a laminated rubber bearing. Polym Test 20:159–166
59. Arayapranee W, Garry LR (2008) A comparative study of the cure characteristics, processability, mechanical properties, ageing, and morphology of rice husk ash, silica and carbon black filled 75 : 25 NR/EPDM blends. J Appl Polym Sci 109:932–941
60. Jacques JE (1985) Rubber Compounding, Rubber Technology and Manufacture, 2nd edn. Blow, CM & Hepburn, C, Butterworths, UK
61. Alipour A, Naderi G, Bakhshandeh GR, Vali H, Shokoohi S (2011) Elastomer Nanocomposites Based on NR/EPDM/Organoclay: Morphology and Properties. Int Polym Process 26:48–55
62. Padmini M, Radhakrishnan CK, Sujith A, Unnikrishnan G, Purushothaman E (2006) Molecular transport of aliphatic hydrocarbons through styrene butadiene rubber/ethylene vinyl acetate blends. J Appl Polym Sci 101:2884–2897
63. Unnikrishnan G, Thomas S (1998) Interaction of crosslinked natural rubber with chlorinated hydrocarbons. Polymer 39:3933–3938
64. Tang CY, Chen DZ, Yue TM, Chan KC, Tsui CP, Yu PHF (2008) Water absorption and solubility of PHBHV/HA nanocomposites. Compos Sci Technol 68:1927–1934
65. Flory PJ, Rehner J (1943) Statistical Mechanics of Cross-Linked Polymer Networks I. Rubberlike Elasticity. J Chem Phys 11:512
66. Sujith A, Unnikrishnan G (2006) Molecular sorption by heterogeneous natural rubber/poly(ethylene-co-vinyl acetate) blend systems. J Polym Res 13:171–180
67. Thomas PC, Tomlal JE, Selvin TP, Thomas S, Joseph K (2010) High-performance nanocomposites based on arcylonitrile-butadiene rubber with fillers of different particle size: Mechanical and morphological studies. Polym Compos 31:1515–1524
68. Naseri ASZ, Jalali-Arani A (2015) A comparison between the effects of gamma radiation and sulfur cure system on the microstructure and crosslink network of (styrene butadiene rubber/ethylene propylene diene monomer) blends in presence of nanoclay. Radiat Phys Chem 115:68–74
69. Noriman NZ, Ismail H (2012) Properties of styrene butadiene rubber (SBR)/recycled acrylonitrile butadiene rubber (NBRr) blends: the effects of carbon black/silica (CB/silica) hybrid filler and silane coupling agent, Si69. J Appl Polym Sci 124:19–27